



# Deletion of *Nrip1* delays skin aging by reducing adipose-derived mesenchymal stem cells (ADMSCs) senescence, and maintaining ADMSCs quiescence

Yu Hu · Yun Zhu · Skyler D. Gerber · Jared M. Osland · Min Chen · Krishna A. Rao · Heng Gu · Rong Yuan 

Received: 11 March 2020 / Accepted: 15 February 2021 / Published online: 11 March 2021  
© American Aging Association 2021

**Abstract** Our previous studies found that deletion of nuclear receptor interacting protein 1 (*Nrip1*) extended longevity in female mice and delayed cell senescence. The current study investigates the role of NRIP1 in regulating functions of adipose-derived mesenchymal stem cells (ADMSCs) and explores the mechanisms of NRIP1 in skin aging. We first verified the skin aging phenotypes in young (6 months) and old (20 months) C57BL/6J (B6) mice and found deletion of *Nrip1* can delay skin aging phenotypes, including reduced thickness of dermis and subcutaneous white adipose tissue (sWAT), as well as the accumulation of senescent cells in sWAT. In ADMSCs isolated from sWAT, we found that deletion of *Nrip1* could decrease cell proliferation, prevent cell apoptosis, and suppress adipogenesis. Interestingly, deletion of *Nrip1* also reduced cell senescence and maintain cell quiescence of ADMSCs. Moreover,

the expressions of genes associated with senescence (*p21*, and *p53*), inflammation (*p65*, *IL6*, and *IL1a*), and growth factor (*mTOR*, *Igf1*) were reduced in *Nrip1* knockout ADMSCs, as well as in *siNrip1*-treated ADMSCs. Suppression of *Nrip1* by *siNrip1* also decreased the expressions of mTOR, p-mTOR, p65, and p-p65 in ADMSCs. Reduced expressions of p65 and p-p65 were also confirmed in the skin of *Nrip1* knockout mice. These findings suggest that NRIP1 plays an important role in delaying skin aging by reducing ADMSCs senescence and maintaining ADMSCs quiescence.

**Keywords** NRIP1 · Skin aging · ADMSC · Senescence · Quiescence

## Introduction

Skin aging is a continuous dynamic process. Clinically, skin aging is mainly manifested as wrinkle formation, loss of elasticity, and pigmentation. Histologically, skin aging is characterized by thinning of epidermis, atrophy of dermis, flattening of the dermoepidermal junction, accumulation of abnormal elastic tissue in the dermis, and reduced amounts of subcutaneous white adipose tissue (sWAT) [43]. Although the pathological mechanism of skin aging is complex, previous studies found that the pathogenesis mainly included mutations of mitochondrial DNA, accumulated oxidative stress, overexpressed matrix metalloproteinases (MMPs), and increased inflammatory reactions [20]. Recently, increasing evidence has shown that sWAT is correlated with intrinsic

---

Y. Hu · Y. Zhu · S. D. Gerber · J. M. Osland · R. Yuan (✉)  
Division of Geriatric Research, Department of Internal Medicine,  
Southern Illinois University School of Medicine, 801 N. Rutledge  
Street Room 4361, Springfield, IL 62702, USA  
e-mail: ryuan@siumed.edu

Y. Hu · M. Chen · H. Gu (✉)  
Institute of Dermatology, Chinese Academy of Medical Sciences  
and Peking Union Medical College, 12 Jiangwangmiao Street,  
Nanjing, Jiangsu, China  
e-mail: guheng@pumcdem.cams.cn

K. A. Rao  
Division of Hematology/Oncology, Department of Internal  
Medicine, Simmons Cancer Institute at Southern Illinois  
University School of Medicine, Springfield, IL, USA

aging, as its structure and volume are significantly altered during the process of aging. The alterations of sWAT structure include reduction of the sWAT thickness, reduction of the number and the proliferative ability of preadipocytes, change of the intercellular matrix, and modification of the size of adipocytes [41]. Notably, adipocytes have an important impact on immune reaction and inflammation. Accumulating evidence suggests that the alteration of function in adipocytes plays an important role in aging-related pathological changes.

Nuclear receptor interacting protein 1 (NRIP1), also known as RIP140 (receptor interacting protein of 140 kDa), regulates gene expression by interacting with nuclear receptors, such as estrogen receptor (ER) and androgen receptor (AR). NRIP1 is highly expressed in adipose tissue, liver, and skeletal muscle, and is involved in metabolism, aging, and other physiological process. Compared to wild-type mice, *Nrip1* knockout mice are lean, have lower body fat content, and are resistant to obesity induced by a high-fat diet [40]. Our previous study found that deletion of *Nrip1* extends longevity of female mice and delays senescence in white adipose tissue (WAT) [40]. We also found that NRIP1 is overexpressed in lesions and peripheral blood mononuclear cells (PBMCs) of psoriasis patients. Suppression of NRIP1 in both CD4+ T cells of psoriasis patients and the IMQ-induced psoriasis-like mouse model can down-regulate the expression of NF $\kappa$ B. Additionally, in macrophages, NRIP1 functions as a co-activator for NF $\kappa$ B through direct interaction with RelA/p65 and upregulates the downstream inflammatory gene expression such as TNF- $\alpha$  and interleukin-6 [44].

To investigate the potential role of NRIP1 in skin aging, we first tested the skin aging phenotypes in young (6 months) and old (20 months) C57BL/6J (B6) mice, as well as in *Nrip1*<sup>+/+</sup> and *Nrip1*<sup>-/-</sup> mice at old age (20 months). We also isolated adipose-derived mesenchymal stem cells (ADMSCs) from sWAT of both *Nrip1*<sup>+/+</sup> and *Nrip1*<sup>-/-</sup> mice and tested the cell phenotypes, including cell senescence, proliferation, apoptosis, and adipogenic differentiation ability. Accordingly, we examined cell cycle and quiescence of ADMSCs to understand the reason why depletion of *Nrip1* can reduce cell senescence. Moreover, we tested the genes associated with senescence (*p16*, *p21*, and *p53*), growth factors (*mTOR* and *Igf1*), and inflammation-related genes (*p65*, *IL6*, and *IL1a*) in ADMSCs and skin to further delineate the mechanism of how NRIP1 regulates ADMSCs in skin aging.

## Materials and methods

**Mice** The C57BL/6J (B6, strain ID 000664) mice were purchased from The Jackson Laboratory. The *Nrip1* global knockout strain (RY-*Nrip1* KO) was created by using the Cre/LoxP strategy described previously [40]. Mice were housed in the Division of Laboratory Animal Medicine at Southern Illinois University School of Medicine (SIU-SOM). All animal experiments were conducted in accordance with NIH guidelines and protocols approved by the SIU-SOM Laboratory Animal Care and Use Committee.

**Tissue collection** Mice were euthanized by cervical dislocation for tissue collection. Skin tissue was collected. Tissues for RNA assay were stored in RNAlater (Invitrogen, Cat. #: AM7020) at -20°C. Tissues for protein assays and senescence-associated  $\beta$ -Gal (SA- $\beta$ -Gal) staining were flash-frozen in dry ice with alcohol and stored at -80°C. Tissues for histology were fixed in 10% formalin.

**SA- $\beta$ -gal staining and histological analysis** Senescent cells were detected by using SA- $\beta$ -gal staining kit (Cell Signaling Technology, Cat. #: 9860) according to the manufacturer's instructions. After SA- $\beta$ -gal staining, tissues were embedded in paraffin blocks and sectioned (4  $\mu$ m thick). Then, slides were stained with hematoxylin (Thermo Scientific, Cat. #: 6765001) and eosin (Acros Organics, Cat. #: 17372-87-1). To analyze SA- $\beta$ -gal positive cells, we randomly selected four vision fields under microscope ( $\times 40$ , Olympus IX71) for each slide and calculated the percentage of positive cells. For measuring thickness of dermis and subcutaneous, as well as the diameter of subcutaneous adipocyte, four pictures were taken randomly for each H&E-stained slide under microscope ( $\times 40$ , Olympus IX71).

**Immunohistochemistry** Immunohistochemistry staining was performed by using Pierce Peroxidase Detection Kit (Thermo Scientific, Cat. #: 36000). In short, antigen retrieval was performed using 10  $\mu$ M citrate buffer (pH=6.0) for 15 min at 90–95°C. After antigen retrieval, sections were treated with peroxidase suppressor to block endogenous peroxidase. Incubation of blocking buffer provided by the kit for 1 h was followed by treatment with primary antibodies at 4°C overnight. Sections were then incubated with secondary antibody HRP polymer-Rabbit IgG (1:100, R&D, Cat. #: VC003-

025), followed by the incubation with secondary antibody, DAB/Metal Substrate Working Solution, for 5–15 min until desired stain. Finally, sections were counterstained with hematoxylin, dehydrated, and mounted. Primary antibody used in this study includes p-NF $\kappa$ B p65 (1:200, Santa Cruz, Cat. #: sc-33039). Since the primary antibody was raised in rabbit, rabbit IgG (1:200, Invitrogen, Cat. #:10500C) was used as false positive control.

**Isolation of ADMSCs and cell culture** Inguinal adipose tissue was obtained from B6, RY-*Nrip1*<sup>+/+</sup>, and RY-*Nrip1*<sup>-/-</sup> female mice at 6 to 8 months of age. After being minced, tissue was digested by collagenase/dispase (1 mg/ml, Sigma, Cat. #: 10269638001) with 10 mM CaCl<sub>2</sub> with constant agitation for 45 min at 37°C. The digestion medium was filtered through a 100- $\mu$ m cell strainer, washed with PBS, and centrifuged at 500g for 10 min. After centrifugation, the cells were filtered through and a 70- $\mu$ m strainer and then resuspended in  $\alpha$ -MEM (Corning, Cat. #: 10-022-CV) supplemented with 10% FBS, 1% penicillin and streptomycin, and 250 ng/ml amphotericin B (Sigma, Cat. #: A2942). Culture medium was changed 2 h after plating the cells, followed by another medium change after 12 h, and then every 2 days. Cells of the first four generations were used in the following studies.

**Flow cytometry** The surface phenotypic characterization of ADMSCs was determined by flow cytometric analysis. Briefly,  $3 \times 10^6$  cells were suspended in 1 ml PBS containing 10% FBS and aliquots of 100  $\mu$ l were incubated with labeled antibodies (purified anti-mouse CD29, CD31, and CD44, Cat. #: MUXMX-09011, Cyagen) for 30 min at 4°C and were washed twice with PBS. Then, cells were incubated with fluorescein isothiocyanate (FITC) or phycoerythrin (PE)-conjugated goat anti-rat IgG secondary antibodies for 30 min at 4°C. Fluorescence of 15,000 viable cells was analyzed using a flow cytometer (FACSCalibur, BD Biosciences, USA).

**siRNA transfection** siCON (Santa Cruz, Cat. #: sc-37007) and siRIP140 (Santa Cruz, Cat. #: sc-36428) were mixed with Lipofectamine 3000 (Life Technologies, Cat. #: L3000-015) and incubated for 45 min at room temperature. Cells were incubated in the transfection medium for 6 h, and then, an equal volume of complete medium was added without removing the

transfection medium. Culture medium was changed after 24 h. At 48, 72, and 96 h post-transfection, cells were stained with SA- $\beta$ -Gal staining or collected for qPCR and western blot analysis

**Cell proliferation assay** MTT (MTT, Sigma, Cat. #: M2003) assay was applied to evaluate cell proliferation. Cells were seeded at the concentration of  $4 \times 10^4$  cells/well in 6-well plates. 100  $\mu$ l of 5 mg/ml 3-(4,5-dimethylthiazol-2-yl)-2,5-diphenyltetrazolium bromide and 1.9 ml serum-free culture medium were added to each well at 24, 48, 72, 96, and 120h after being seeded. Following 4-h incubation, wells were aspirated and 1 ml of MTT solvent (4 mM HCl, 0.1% Nondet P-40 (NP40) all in isopropanol) was added to each well. After being resolved completely, solution of each well was aliquoted to four wells of a 96-well plate (250 $\mu$ l/well), and the concentration of cells was calculated by the absorptions at 570 nm and 690nm measured by spectrophotometry (BioTek PowerWave XS, Winooski).

**Examination of cumulative population doubling level** ADMSCs were isolated from female *Nrip1*<sup>+/+</sup> and *Nrip1*<sup>-/-</sup> mice at middle age (13months). The ADMSCs were seeded at a density of  $3 \times 10^4$  cells per well in a 6-well cell culture plate and maintained for 5 days. Cells were passaged every 5 days with trypsinization and replated at the same density ( $3 \times 10^4$  cell/well) for the cumulative population doubling level (cPDL). During continuous passages, the numbers of ADMSCs at both the seeding and harvesting times were determined to calculate the cPDL. We calculated cPDL using the formula:  $cPDL = \log(n_f/n_0)/\log 2 + X$ , where  $n_0$  is the initial number of cells at the beginning of the subculture, and  $n_f$  the final number of cells at the end of that subculture.  $X$  is the doubling level of the cells at the initiation of the subculture.

**Cell apoptosis assay** Annexin-V staining was applied to evaluate cell apoptosis. The cells were stained with PE Annexin-V and 7-Amino-Actinomycin (7-AAD) following the manufacturer's instructions (BD Pharmingen, Franklin Lakes). The percentage of live (PE Annexin-V-/7-AAD-), apoptotic (PE Annexin-V+/7-AAD-), and necrotic (PE Annexin-V+/7-AAD+) cells was analyzed with flow cytometry (BD Accuri C6).

**Cell cycle assays** Propidium iodide (PI; BD Pharmingen, Franklin Lakes) staining was applied to

determine cell cycle. Cells were fixed in 75% ethanol overnight at 4°C, then stained with PI (50 µg/ml) containing RNase A (16 µg/ml), and incubated for 45 min at 37°C. For each sample, at least 30,000 events were collected and examined by flow cytometry (BD Accuri C6).

**Adipogenic differentiation of ADMSCs** The potential of cultured ADMSCs to differentiate into adipocytes was determined. Cells were cultured in 35-mm dishes until 100% confluent, and then, the differentiation was induced by completed StemXVivo adipogenic differentiation media (1:100 dilution of StemXVivo® Adipogenic Supplement in  $\alpha$ -MEM; R&D, Cat. #: CCM011). Oil Red O (Sigma, Cat. #: O0625) staining was used to detect intracellular lipid droplets after 4-, 8-, and 12-day induction.

**Cell senescence** For detecting senescence, ADMSCs were seeded in 6-well plates at the concentration of  $5 \times 10^3$  cells/well. At days 5, 7, 9, and 11, cells were stained by SA- $\beta$ -gal. To quantitate the SA- $\beta$ -gal positive cells, after staining with DAPI, 4 random vision fields were selected under microscope ( $\times 40$ ) for each well and the percentage of positive cells was calculated.

**Immunocytochemistry** Cells were stained with 4% paraformaldehyde in PBS (pH 7.5) at room temperature for 15 min. Then, cells were permeabilized with 0.3% Triton X-100 in PBS for 5 min at room temperature. After blocking with 5% BSA for 1 h, cells were incubated with primary antibody against Ki67 (1:100; Novus Biologicals, Cat. #: NB600-1209) at 4°C overnight. After washing, cells were reacted with chicken anti-rabbit IgG (H+L) secondary antibodies (FITC; Novex life technologies, Invitrogen, Cat. #: A15988). Nuclei were stained with NucBlue™ Live Cell Stain (life technologies, Invitrogen, Cat. #: R37605). Images were captured using a Zeiss LSM800 scanning confocal microscope (Carl Zeiss, Jena, Germany). The total numbers of cells and Ki67-positive cells were counted and the percentage of Ki67-positive cells was calculated.

**RNA extraction and qRT-PCR** Total RNA was isolated by TRIzol Reagent (Sigma, Cat. #: T9424). Complementary DNA was synthesized using the All-in-One

cDNA Synthesis SuperMix (Bioutil, Cat. #: B24403). One micrograms of total RNA was reverse transcribed in 10µl reaction following the manufacturer's instructions. qRT-PCR was performed using the SYBR Green One Step qPCR Kit (Bioutil, Cat. #: B21202) on the ABI 7500 Real-Time PCR machine (Applied Biosystems). Primers used for qPT-PCR are listed in Table 1.

**ELISA** The level of IL-6 in culture medium was evaluated using ELISA kit (Thermo Scientific, Cat. #: 88-7064-22), according to the protocol provided by the manufacturer.

**Protein extraction and western blot** Skin tissues were homogenized in ice-cold homogenization buffer (50mM Tris HCL pH 8.0, 0.5mM DTT, 0.1% NP-40) in the presence of protease/phosphatase inhibitor using a handheld pestle. After homogenization, tissues were lysed in RIPA buffer (20mM Tris HCL pH 8.0, 300 mM NaCl, 1 mM DTT, 2% NP-40, 1% sodium deoxycholate, 0.2% SDS) containing Halt™ Protease and Phosphatase Inhibitor Cocktail (Thermo Scientific, Cat. #: 78440) for 1 h on ice. Protein was obtained after centrifugation for 20 min at 12,000 $\times g$  at 4°C. Protein concentration was measured by Pierce BCA Concentration Test Kit (Thermo Scientific, Cat. #: 23225). Protein samples were heat-denatured in Laemmli Loading Buffer (Alfa Aesar, J60660-AC) with 1%  $\beta$ -ME. 20–40 µg protein was separated on sodium dodecylsulfate-polyacrylamide gel (SDS-PAGE) and transferred to a 0.22-µm polyvinylidene difluoride membrane (NEN LifeScience Products). Non-specific binding sites were blocked with 5% BSA in TBST. After blocking, the membranes were incubated overnight at 4°C with primary antibody against NF $\kappa$ B (1:200, Santa Cruz, Cat. #: sc-8008), p-NF $\kappa$ B (1:500, Santa Cruz, Cat. #: sc-33039), and GAPDH (1:2000, CST, Cat. #: 2118S). Immune complexes were detected with RDye 800CW goat anti-rabbit IgG (LiCor, Cat. #: C30521-01) and the intensity of protein bands was quantified using an Odyssey Infrared Imaging System (LiCOR).

**Statistical analysis** All data are shown as means  $\pm$  standard errors (SE). Data were analyzed by two-tailed Student's *t* test.  $P < 0.05$  was considered as a statistically significant difference.

**Table 1** Primer sequences used for qRT-PCR

Gene	Forward primer sequence (5'-3')	Reverse primer sequence (5'-3')
<i>Adiponection</i>	TATCGCTCAGCGTTCAGTGT	AGAGTCCCGGAATGTTGCAG
<i>Fabp4</i>	CGATGAAATCACCGCAGACG	CCAGCTTGTCCACCATCTCGT
<i>Gapdh</i>	ATGTGTCCGTCGTGGATCTGAC	AGACAACCTGGTCCTCAGTGAG
<i>Igfl</i>	TGCTCTTCAGTTCGTGTG	ACATCTCCAGTCTCCTCAG
<i>IL1a</i>	TGCAGTCCATAACCCATGATC	ACAAACTTCTGCCTGACGAG
<i>IL6</i>	CAAAGCCAGAGTCCTCAGAGAG	GCCACTCCTTCTGTGACTCC
<i>mTOR</i>	TGCTTGTTGGTTGGCATAACA	TTCAGAGCCACAAACAGAGC
<i>Nrip1</i>	AGCAGGACAAGAGTCACAGAAAC	TGTGATGATTGGCAGTATCTACG
<i>p16</i>	GTGTGCATGACGTGCGGG	GCAGTTCGAATCTGCACCGTAG
<i>p21</i>	AACATCTCAGGGCCGAAA	TGCGCTTGGAGTGATAGAAA
<i>p53</i>	CTAGCATTACAGGCCCTCATCC	TCCGACTGTGACTCCTCCAT
<i>p65</i>	CTTGGAACAGCACAGACC	GAGAAGTCCATGTCCGCAAT
<i>Ppar<math>\gamma</math></i>	GTGAGACCAACAGCCTGAC	TATCAGTGGTTCACCGCTTC

## Results

### Skin aging phenotypes in young and old B6 mice

To verify skin aging phenotypes in B6 mice, dorsal skin sections of young (6-month-old,  $n=4$ ) and old (20-month-old,  $n=4$ ) female B6 mice were subjected to histopathological analysis. The thickness of dermis and subcutaneous white adipose tissue (sWAT) from old mice was reduced significantly compared to young mice ( $168.50\pm 13.89\mu\text{m}$  vs.  $229.56\pm 14.80\mu\text{m}$ ,  $P=0.040$ ,  $257.55\pm 54.43\mu\text{m}$  vs.  $436.42\pm 31.59\mu\text{m}$ ,  $P=0.046$ , Fig. 1a, b). Moreover, the diameter of subcutaneous adipocyte from old mice was significantly reduced compared to young mice ( $33.06\pm 1.12\mu\text{m}$  vs.  $43.09\pm 1.55\mu\text{m}$ ,  $P=0.006$ , Fig. 1c). Importantly, the number of senescent cells, detected by SA- $\beta$ -gal staining, in sWAT of old mice was over five times more than that of young mice ( $71.51\pm 1.71\%$  vs.  $14.65\pm 1.29\%$ ,  $P<0.001$ , Fig. 1a, d)

### Depletion of *Nrip1* alters skin aging phenotypes

To investigate the role of NRIP1 in skin aging, we collected skin tissues from female *Nrip1*<sup>+/+</sup> ( $n=3$ ) and *Nrip1*<sup>-/-</sup> ( $n=4$ ) mice at the age of 20 months. We measured the thickness of dermis and sWAT, as well as the percentage of SA- $\beta$ -gal positive adipocytes. The results showed that the thickness of dermis and sWAT is significantly increased in *Nrip1*<sup>-/-</sup> mice compared with *Nrip1*<sup>+/+</sup> mice ( $214.68.50\pm 15.38\mu\text{m}$  vs.  $152.82$

$\pm 5.46\mu\text{m}$ ,  $P=0.036$ ,  $427.72\pm 22.27\mu\text{m}$  vs.  $230.30\pm 9.34\mu\text{m}$ ,  $P=0.0028$ , Fig. 2a, b). The diameter of subcutaneous adipocyte from *Nrip1*<sup>-/-</sup> mice and *Nrip1*<sup>+/+</sup> mice showed no difference ( $37.50\pm 0.40\mu\text{m}$  vs.  $39.24\pm 2.57\mu\text{m}$ ,  $P=0.66$ , Fig. 2c). The percentage of SA- $\beta$ -gal positive cells was significantly decreased in *Nrip1*<sup>-/-</sup> mice ( $41.86\pm 6.04\%$  vs.  $71.26\pm 2.38\%$ ,  $P=0.02$ , Fig. 2a, d).

### Phenotypic characterization of ADMSCs

As previously described, we isolated ADMSCs from inguinal adipose tissue in B6 mice. The cells were cultured to passage 3 and exhibited a fibroblast-like morphology when reaching full confluence (Fig. 3a). After maintaining in the complete StemXVivo adipogenic differentiation media for 14 days, cells differentiated into adipocytes with lipid vesicle (Fig. 3b). Oil Red O staining also confirmed the adipogenic differentiation of ADMSCs (Fig. 3c). The immunophenotypic characteristics of ADMSCs were analyzed by flow cytometry. The FACS results showed that ADMSCs were positive for CD29 and CD44 and negative for CD31 (Fig. 3d).

### Depletion of *Nrip1* reduces ADMSCs senescence

After isolating ADMSCs from sWAT of *Nrip1*<sup>+/+</sup> and *Nrip1*<sup>-/-</sup> mice at young age (6 months), cell senescence was performed to evaluate the senescent

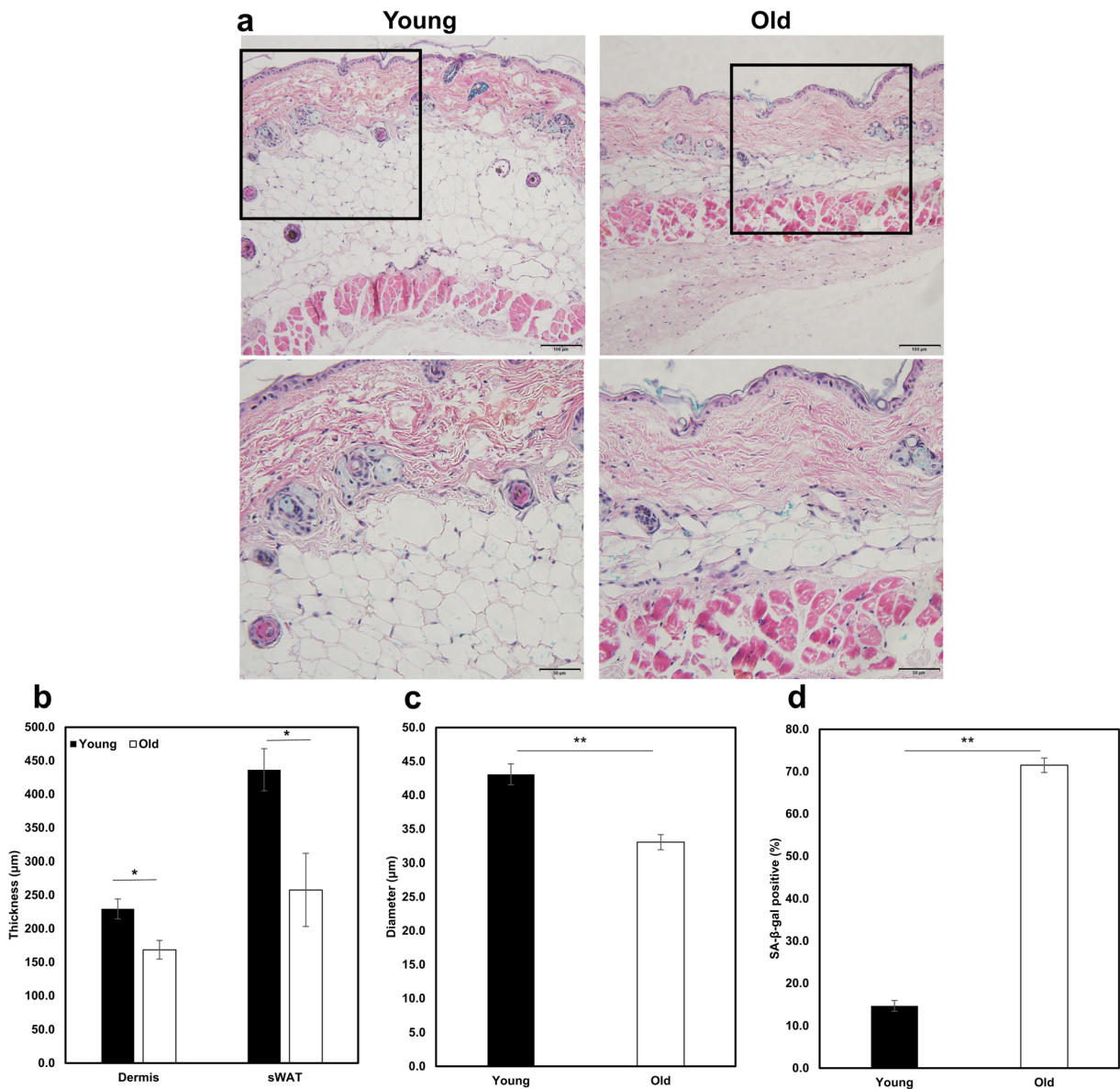


**Fig. 1** Skin aging phenotypes in young and old B6 mice. **a** Dermal and subcutaneous white adipose tissue (sWAT) thickness decreases and senescence increases with age (upper scale bar 100μm, down scale bar 50μm). **b** Quantification of the dermal

and sWAT thickness in young and old mice. **c** Quantification of the subcutaneous adipocyte diameter in young and old mice. **d** The percentage of senescent cells was calculated by SA-β-gal staining. \* $P < 0.05$ , \*\* $P < 0.01$

property. Cell senescence data showed that the number of SA-β-gal positive cells accumulated with culture time in both *Nrip1*<sup>+/+</sup> and *Nrip1*<sup>-/-</sup> ADMSCs. Importantly, the percentage of SA-β-gal positive cells from *Nrip1*<sup>-/-</sup> ADMSCs was significantly lower than that from *Nrip1*<sup>+/+</sup> ADMSCs in day 7, day 9, and day 11 ( $P = 0.028$ ,  $P = 0.0005$ , and  $P = 0.009$ , Fig. 4a, b). To further confirm the role of NRIP1 in regulating senescence in ADMSCs and explore a

potential therapeutic method to delay stem cell senescence, ADMSCs isolated from B6 mice were treated with either siRNA targeting *Nrip1* (*siNrip1*) or siRNA scramble control (*siCon*) on day 4 post-isolation. SA-β-gal staining was performed at 72 h after treatment. The data showed that *siNrip1*-treated group had a significantly lower percentage of senescent cells compared to the *siCon* group (15.3% vs. 23.7%,  $P = 0.034$ , Fig. 4c, d).

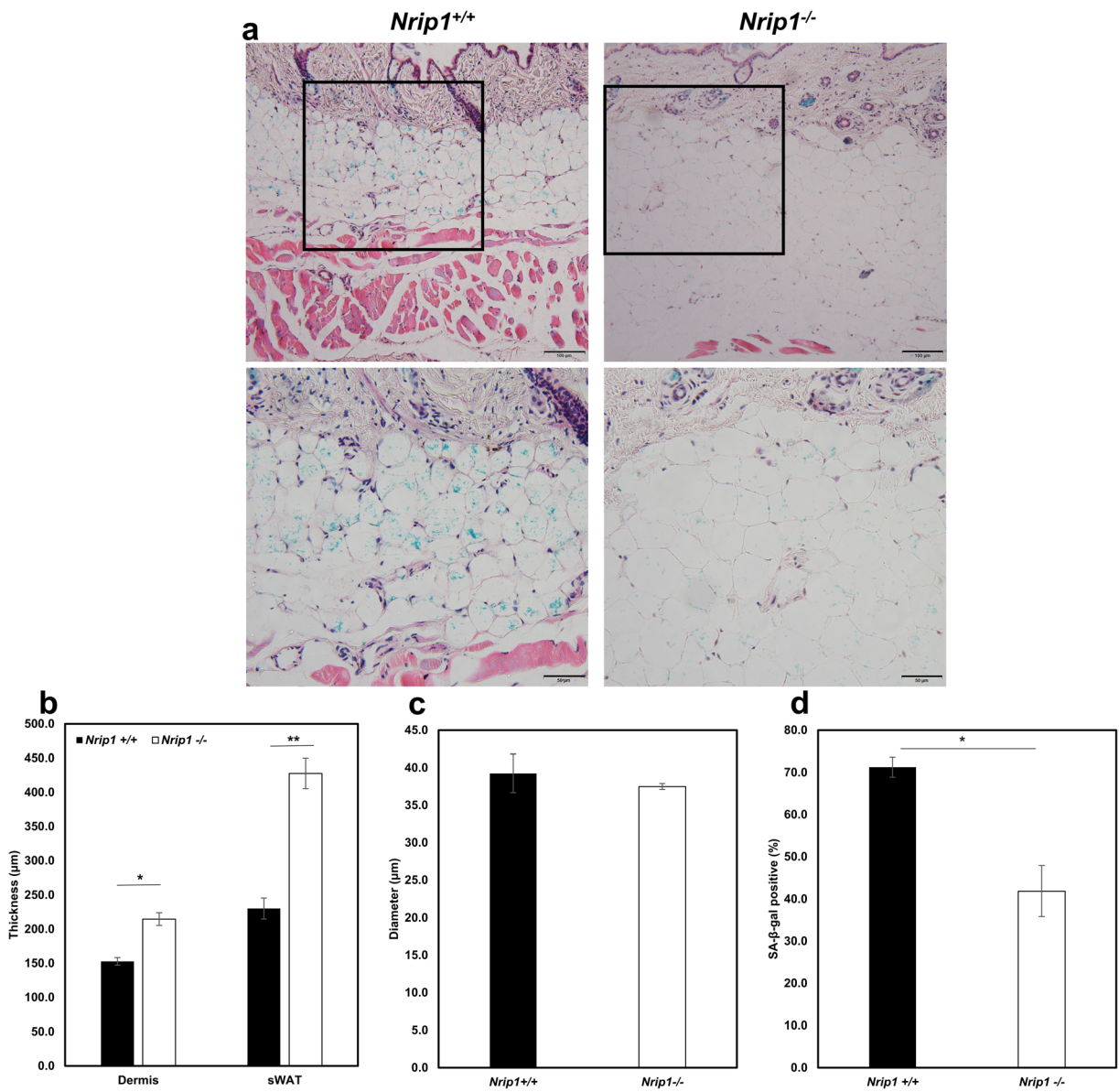


**Fig. 2** Skin aging phenotypes in *Nrip1*<sup>+/+</sup> and *Nrip1*<sup>-/-</sup> mice. **a** Dermal and sWAT thickness decreases and senescence increases in *Nrip1*<sup>-/-</sup> mice (upper scale bar 100μm, down scale bar 50μm). **b** Quantification of the dermal and sWAT thickness in *Nrip1*<sup>+/+</sup> and

*Nrip1*<sup>-/-</sup> mice. **c** Quantification of the subcutaneous adipocyte diameter in *Nrip1*<sup>+/+</sup> and *Nrip1*<sup>-/-</sup> mice. **d** The percentage of senescent cells was calculated by SA-β-gal staining. \**P*<0.05, \*\**P*<0.01

### Depletion of *Nrip1* alters cell proliferation and cell apoptosis of ADMSCs

To verify whether depletion of *Nrip1* alters cell proliferation, cell apoptosis, and colony formation of ADMSCs, we performed MTT assay and Annexin-V staining. As the MTT assay showed, the proliferation rate of *Nrip1*<sup>-/-</sup> ADMSCs was significantly lower than that of *Nrip1*<sup>+/+</sup> ADMSCs

at day 2 and day 4 after being seeded (*P*=0.029 and *P*= 0.012, Fig. 5a). The Annexin-V staining results showed that the percentage of apoptotic cells decreased significantly in *Nrip1*<sup>-/-</sup> ADMSCs compared with *Nrip1*<sup>+/+</sup> ADMSCs at 24, 48, and 72 h after the cells being seeded (*P*<0.001, Fig. 5b). Taken together, these data indicated that depletion of *Nrip1* could decrease cell proliferation and prevent cell apoptosis.

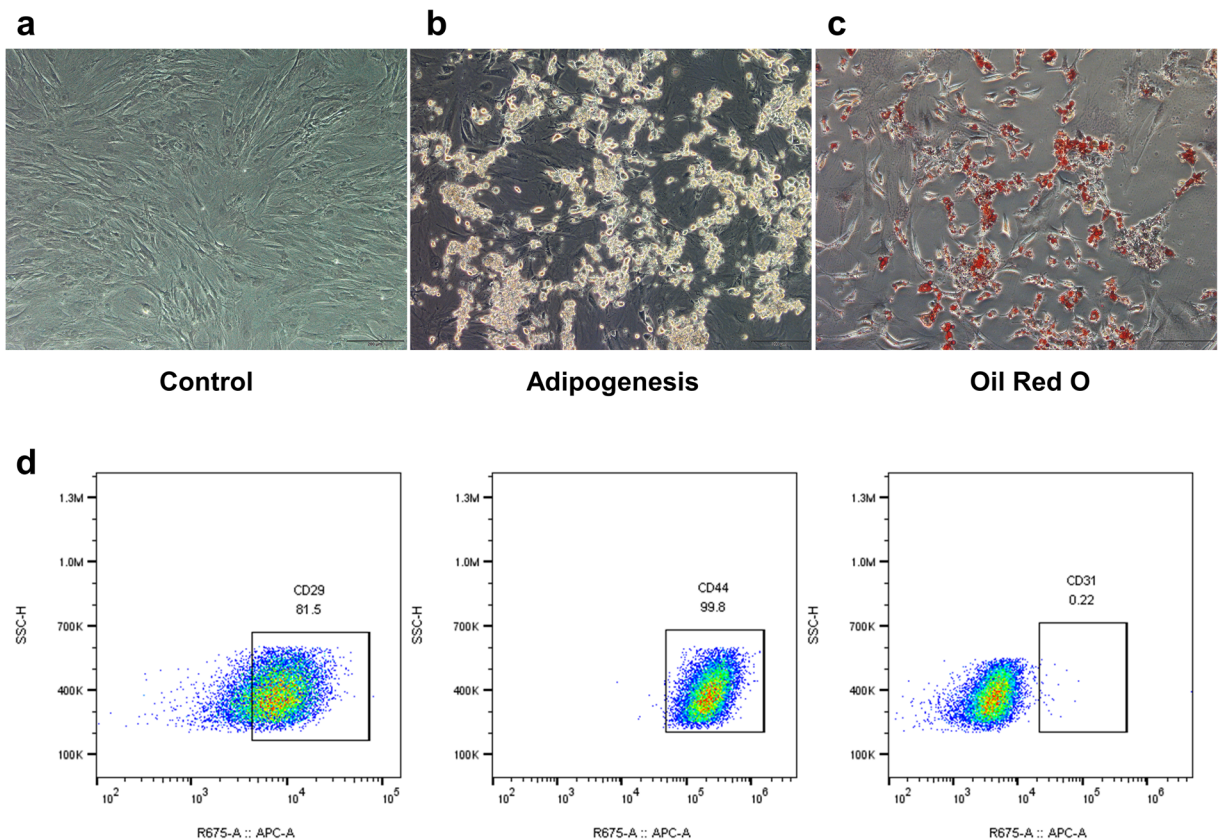


**Fig. 3** Phenotypic characterization of ADMSCs. **a** Morphological feature of ADMSCs at full confluence (scale bar 200 $\mu$ m). **b** Adipogenic differentiation of ADMSCs after 14 days (scale bar 200 $\mu$ m). **c** Adipogenesis was confirmed in ADMSCs by Oil Red

O staining (scale bar 100 $\mu$ m). **d** Detection of MSC-specific marker (CD29+, CD44+, and CD31-) of ADMSCs by flow cytometric analysis

#### Depletion of *Nrip1* delay adipogenic differentiation of ADMSCs

To assess the adipogenic differentiation ability of ADMSCs from *Nrip1*<sup>-/-</sup> and *Nrip1*<sup>+/+</sup> mice, differentiation was induced by culturing with adipogenic differentiation media. Lipid dye Oil Red O was performed to confirm adipogenesis. Starting from day 4, lipid droplets could be observed under a microscope and gradually increased with culture time (Fig. 6a). The result of semi-quantitative detection showed that the absorbance values in *Nrip1*<sup>-/-</sup> ADMSCs were significantly lower compared to *Nrip1*<sup>+/+</sup> ADMSCs at days 8 and 12 ( $P=0.013$  and  $P=0.001$ , Fig. 6b). To quantify the adipogenic differentiation of ADMSCs, genes related to adipogenic differentiation (*Fabp4*, *Ppar* $\gamma$ , and *Adiponectin*) were examined at days 4, 8, and

12 after induction (Fig. 6c). Consistent with Oil Red O staining, the expressions of *Fabp4*, *Ppar* $\gamma$ , and *Adiponectin* were significantly lower in *Nrip1*<sup>-/-</sup> ADMSCs compared to *Nrip1*<sup>+/+</sup> ADMSCs at days 8 and 12. These results suggested that *Nrip1*<sup>-/-</sup> ADMSCs exhibited lower response to induction factors, indicating that depletion of *Nrip1* could suppress the differentiation of ADMSCs.

#### Depletion of *Nrip1* enhances cellular quiescence of ADMSCs

PI staining and flow cytometry assay showed that the percentage of G0/G1 cells was significantly increased in *Nrip1*<sup>-/-</sup> ADMSCs ( $P<0.01$ , Fig. 7a, b). Moreover, compared to *Nrip1*<sup>+/+</sup> ADMSCs, the percentages of both S and G2/M cells were significantly reduced in *Nrip1*<sup>-/-</sup> ADMSCs ( $P<0.05$ , Fig. 7a, b). To further identify the

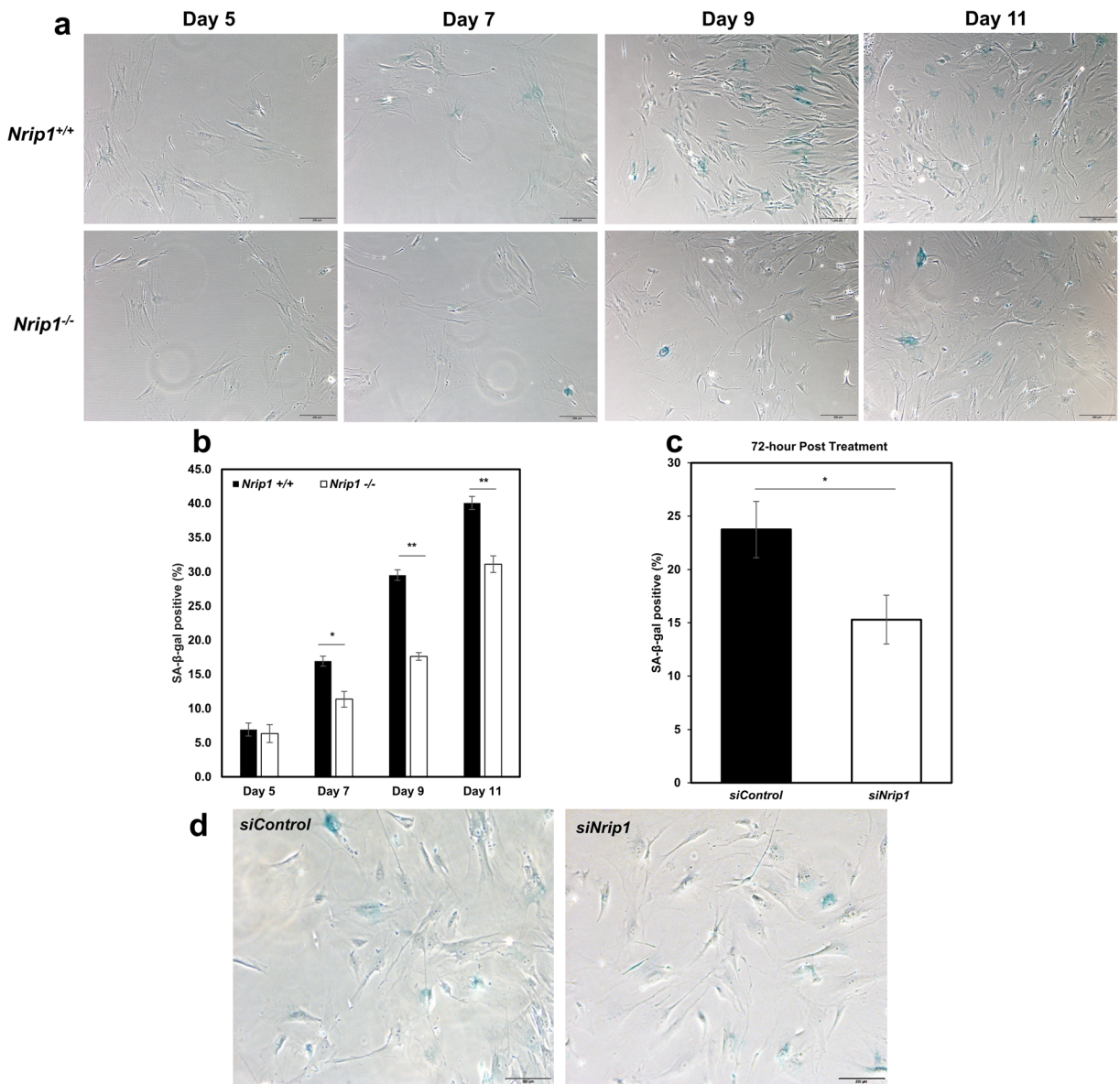


**Fig. 4** Depletion of *Nrip1* reduces ADMSCs senescence. **a** Cell senescence was examined in ADMSCs isolated from *Nrip1*<sup>+/+</sup> and *Nrip1*<sup>-/-</sup> mice at days 5, 7, 9, and 11 (scale bar 100μm). **b** Quantification of SA-β-gal positive cells in *Nrip1*<sup>+/+</sup> and *Nrip1*<sup>-/-</sup> ADMSCs. **c** Quantification of SA-β-gal positive cells in *siCon*

and *siNrip1* ADMSCs isolated from B6 mice at 72 h after treatment. **d** Cell senescence was examined by SA-β-gal staining in *siCon* and *siNrip1* ADMSCs at 72 h after treatment. \**P*<0.05, \*\**P*<0.01

quiescent cell population, immunocytochemistry was performed to stain cells with Ki67. Cells without Ki67 staining were identified as quiescent cells (Fig. 7c). As expected, the percentage of Ki67-positive cells in *Nrip1*<sup>-/-</sup> ADMSCs was significantly lower compared to *Nrip1*<sup>+/+</sup> ADMSCs, indicating that depletion of NRIP1 sustains quiescence of ADMSC (*P*<0.001, Fig. 7d).

Cell phenotypes of ADMSCs from middle age *Nrip1*<sup>+/+</sup> and *Nrip1*<sup>-/-</sup> mice

The cPDL showed that the proliferation rate of *Nrip1*<sup>-/-</sup> ADMSCs at middle age was significantly higher than that of *Nrip1*<sup>+/+</sup> ADMSCs (Fig. 8a). The expression of p21 and p53 was significantly lower in *Nrip1*<sup>-/-</sup>

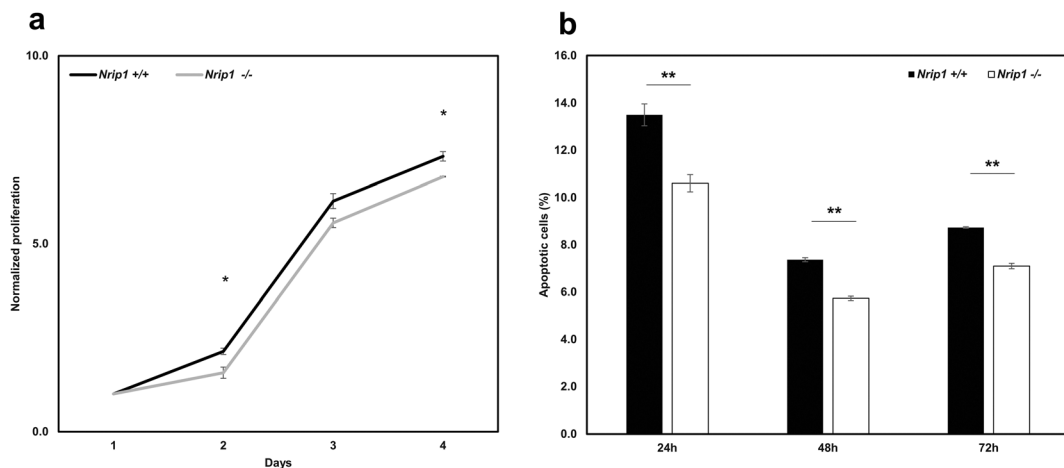


**Fig. 5** Depletion of *Nrip1* alters cell proliferation and cell apoptosis of ADMSCs. **a** MTT assay showed the proliferation rate decreased significantly in *Nrip1*<sup>-/-</sup> ADMSCs compared to *Nrip1*<sup>+/+</sup> ADMSCs at day 2 and day 4 after being seeded. **b** Annexin V

showed that depletion of *Nrip1* inhibited the apoptosis of ADMSCs at 24, 48, and 72 h after being seeded. \* $P < 0.05$ , \*\* $P < 0.01$

ADMSCs compared to *Nrip1*<sup>+/+</sup> ADMSCs at passage 3 ( $P < 0.05$ , Fig. 8b). ELISA result showed that the level of IL-6 was also significantly lower in *Nrip1*<sup>-/-</sup> ADMSCs compared to *Nrip1*<sup>+/+</sup> ADMSCs at passage 3 ( $P < 0.05$ , Fig. 8c). These cell phenotypes results suggested that *Nrip1*<sup>+/+</sup> ADMSCs at middle age began senescing earlier than *Nrip1*<sup>-/-</sup> ADMSCs.

#### Depletion of *Nrip1* alters expression of senescence- and inflammation-associated genes

To investigate the molecular role of NRIP1 in cell senescence, we tested the expression of genes associated with senescence (*p16*, *p21*, and *p53*), growth factors (*mTOR* and *Igf1*), and senescence-associated secretory phenotype (SASP) (*IL6* and *IL1a*). First, the efficiency of knocking out and knocking down *Nrip1* was confirmed by testing the expression of *Nrip1* ( $P < 0.05$ , Fig. 9a, b). The qRT-PCR results showed a 95% depletion of *Nrip1* expression in *Nrip1*<sup>-/-</sup> ADMSCs ( $1.00 \pm 0.28$  vs.  $0.05 \pm 0.03$ , *Nrip1*<sup>+/+</sup> vs. *Nrip1*<sup>-/-</sup>,  $P = 0.015$ ). Comparing to *siCon*, *siNrip1* suppressed 60% of *Nrip1* expression in ADMSCs ( $1.00 \pm 0.09$  vs.  $0.40 \pm 0.04$ , *siCon* vs. *siNrip1*,  $P = 0.026$ ). The expression of senescence-associated genes (*p21* and *p53*) and SASP (*IL6* and *IL1a*) decreased in both *Nrip1*<sup>-/-</sup> and *siNrip1* ADMSCs compared to *Nrip1*<sup>+/+</sup> and *siCon* ADMSCs. However, the expression of *p16* increased in *Nrip1*<sup>-/-</sup> ADMSCs compared to *Nrip1*<sup>+/+</sup> ADMSCs. Moreover, gene expression results showed that *Igf1*, *mTOR*, and *p65* were

all significantly reduced in *Nrip1*<sup>-/-</sup> and *siNrip1* ADMSCs (Fig. 9a, b). Consistently, the western blot results showed that at protein level, mTOR, p65, and p-p65 were significantly lower in *siNrip1* ADMSCs than in *siCon* ADMSCs, while p-mTOR showed suggestively lower in *siNRIP1* ADMSCs ( $P = 0.08$ , Fig. 9c, d).

#### Depletion of *Nrip1* reduces p-p65 level in skin

In order to confirm whether depletion of *Nrip1* would regulate the expression of *p65* in skin, expressions of *Nrip1*, *p65*, *mTOR*, and *Igf1* in mRNA levels were measured by qRT-PCR in the skin of *Nrip1*<sup>-/-</sup> and *Nrip1*<sup>+/+</sup> mice. The reduced expression of *Nrip1* confirmed the successful knockout of *Nrip1* in skin. Consistent with the results of ADMSCs, expressions of *mTOR* and *Igf1* were significantly reduced in the skin of *Nrip1*<sup>-/-</sup> mice ( $P < 0.001$  and  $P < 0.032$ , Fig. 10a). The results showed that *p65* expression in the skin was suggestively reduced in *Nrip1*<sup>-/-</sup> mice compared to *Nrip1*<sup>+/+</sup> mice ( $P = 0.12$ , Fig. 10a). In western blot results, p-p65 was significantly reduced in the skin of *Nrip1*<sup>-/-</sup> mice ( $P = 0.048$ , Fig. 10b), while p65 was suggestively reduced. We also performed immunohistochemistry to verify the level of p-p65 in young (6-month-old) and old (20-month-old) B6 mice, as well as *Nrip1*<sup>+/+</sup> and *Nrip1*<sup>-/-</sup> mice at old age (20-month-old). Increased p-p65 levels were seen in the sWAT at old age (Fig. 10c). Moreover, p-p65 levels were reduced in *Nrip1*<sup>-/-</sup> mice compared with *Nrip1*<sup>+/+</sup> mice (Fig. 10c).

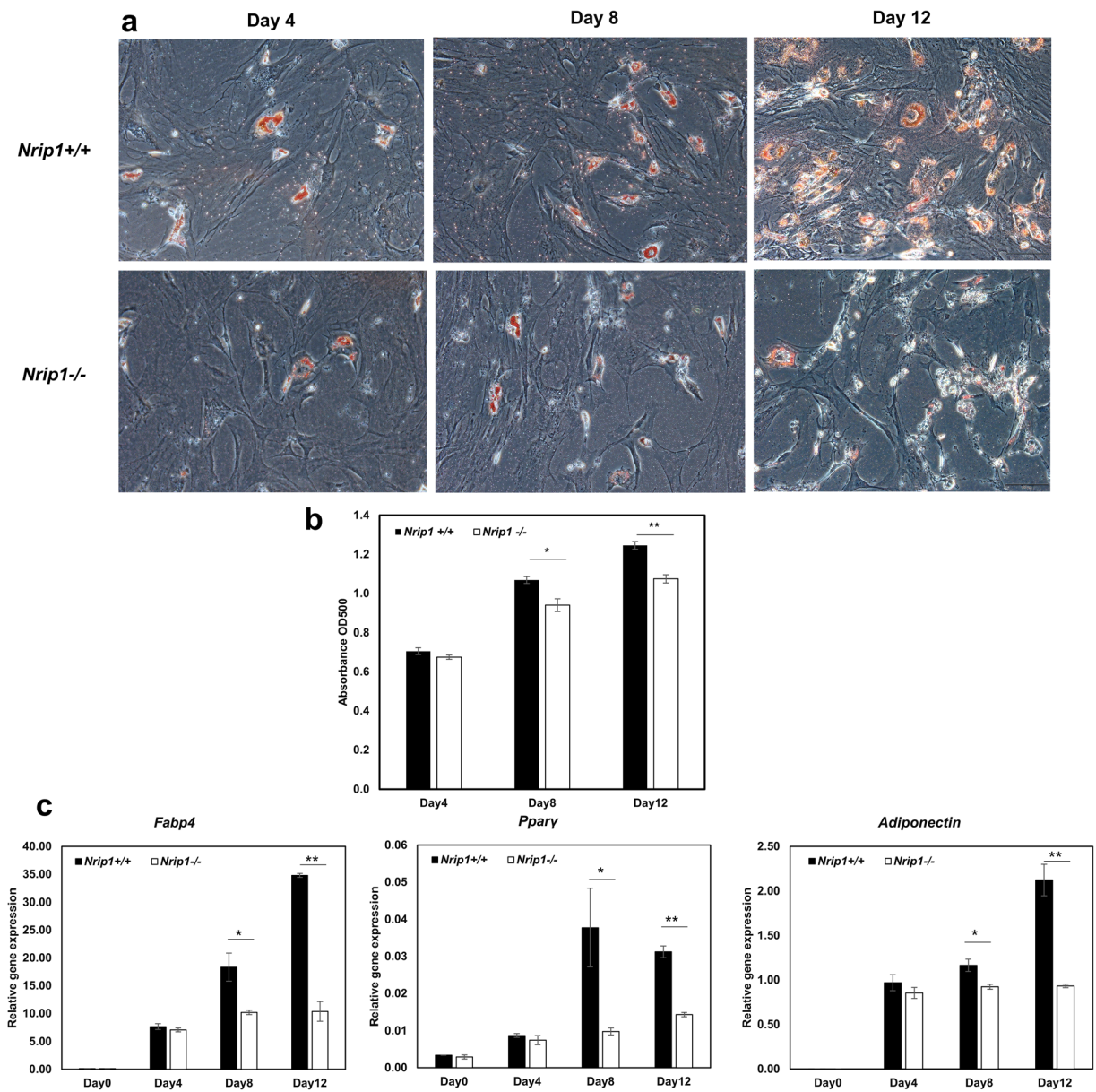


**Fig. 6** Adipogenic differentiation in *Nrip1*<sup>+/+</sup> and *Nrip1*<sup>-/-</sup> ADMSCs. **a** Adipogenesis was detected by Oil Red O staining in *Nrip1*<sup>+/+</sup> and *Nrip1*<sup>-/-</sup> ADMSCs at 4, 8, and 12 days after induction. **b** Semi-quantitative detection of adipogenesis showed

that the absorbance values in *Nrip1*<sup>-/-</sup> ADMSCs were significantly lower compared to *Nrip1*<sup>+/+</sup> ADMSCs at days 8 and 12. **c** Genes related to adipogenic differentiation (*Fabp4*, *Pparγ*, and *Adiponectin*) were analyzed by qRT-PCR. \**P*<0.05, \*\**P*<0.01

## Discussion

NRIP1 acts as a co-regulator by interacting with other nuclear receptors and transcription factors [2]. Using bioinformatics and genetic strategies, a previous study suggested that *NRIP1* might be a strong candidate aging-related gene [7]. It is reported that NRIP1 might be involved in the aging process by suppressing

mitochondrial biogenesis via regulating peroxisome proliferator-activated receptor gamma coactivator-1 $\alpha$  (PGC-1  $\alpha$ ) [25]. Moreover, the expression of NRIP1 in liver, kidney, and adipose tissue showed age-specific changes [10]. Most importantly, our group found deletion of *Nrip1* extended longevity in female mice and delayed senescence of mouse embryonic fibroblasts (MEFs), indicating that NRIP1 plays an important role in aging [40].

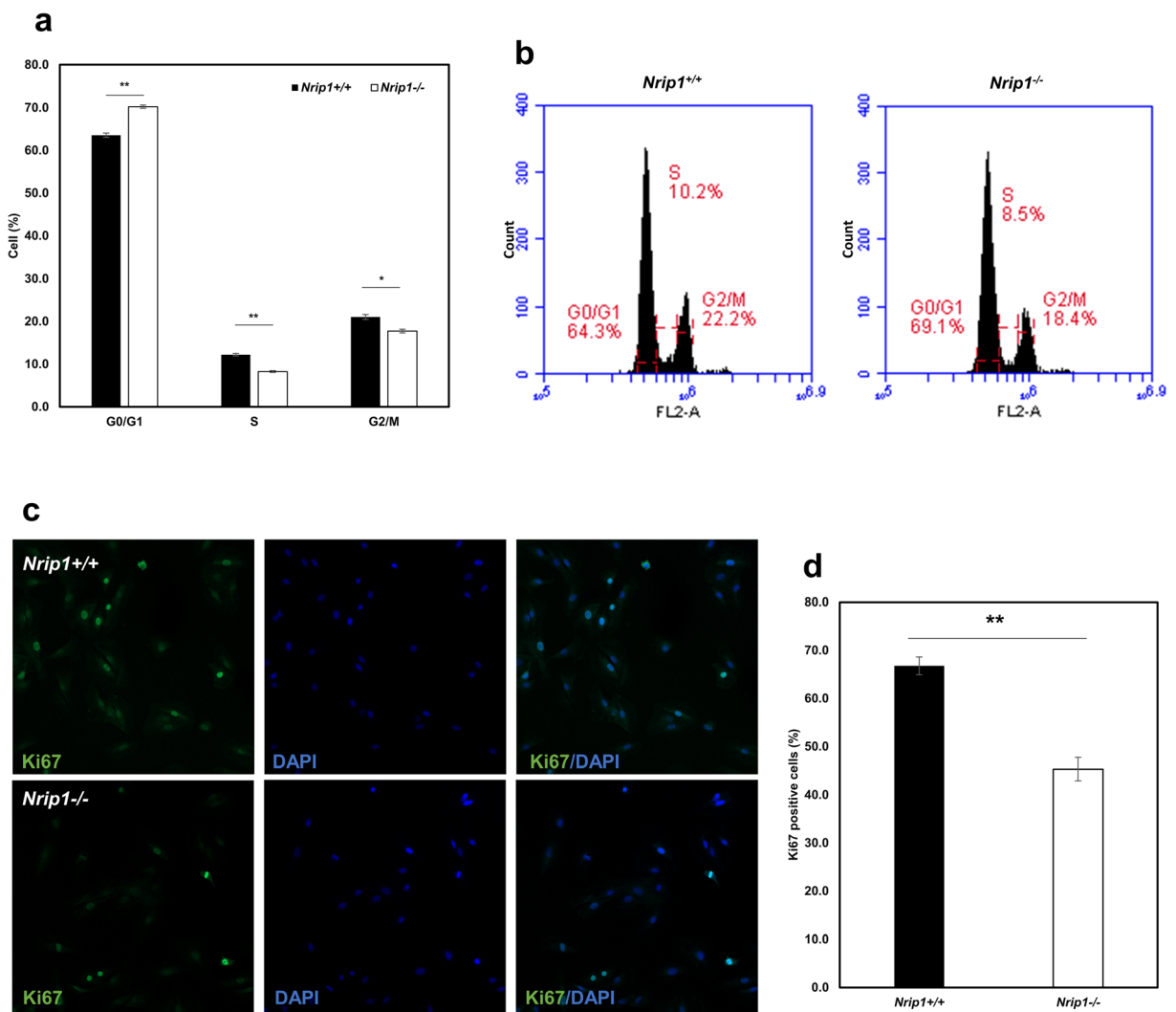


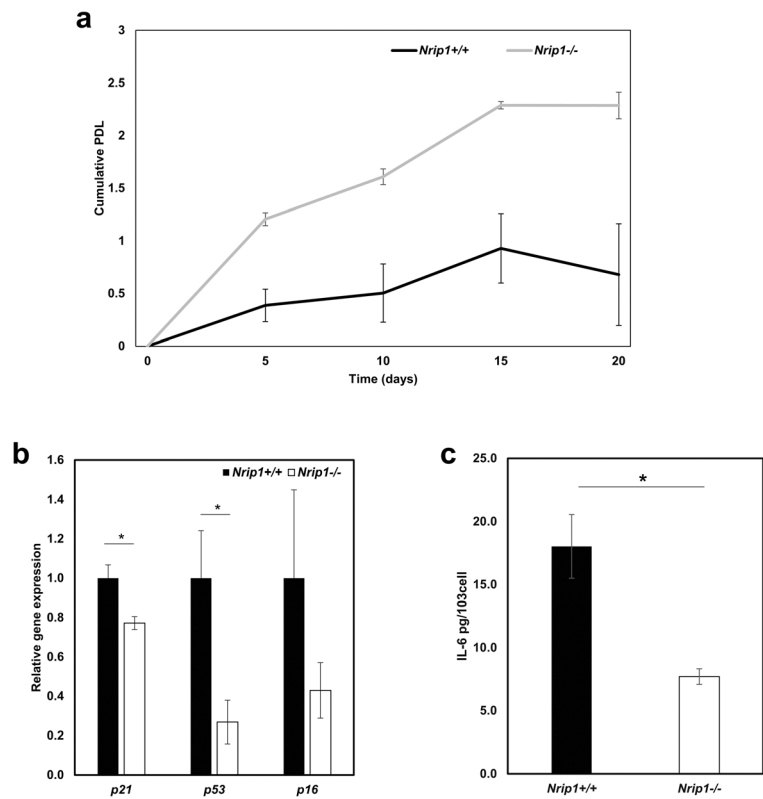
**Fig. 7** Depletion of *Nrip1* enhances cellular quiescence of ADMSCs. **a**, **b** Cell cycle distribution of ADMSCs in *Nrip1*<sup>+/+</sup> and *Nrip1*<sup>-/-</sup> ADMSCs. **c** Ki67-positive cells were presented by

immunocytochemistry in *Nrip1*<sup>+/+</sup> and *Nrip1*<sup>-/-</sup> ADMSCs. **d** Quantification of Ki67-positive cells in *Nrip1*<sup>+/+</sup> and *Nrip1*<sup>-/-</sup> ADMSCs. \* $P < 0.05$ , \*\* $P < 0.01$

To our knowledge, this is the first study to evaluate the role of NRIP1 in skin aging. Previous studies in mice found some common histologic characteristics of skin aging that is also found in the human, including atrophy of dermis, loss of subcutaneous fat, graying of hair, and alopecia [12, 18]. In our study, we verified that the thickness of dermis and sWAT and the diameter of subcutaneous adipocyte in old B6 mice are significantly reduced compared to young B6 mice, which is in accordance with other previous studies [12, 35, 41]. Also, the current study found that the deletion of *Nrip1* could significantly improve some skin aging phenotypes,

including the increased thickness of dermis and sWAT, as well as reduced accumulation of senescent adipocytes. Nevertheless, the diameter of subcutaneous adipocyte showed no difference in old *Nrip1*<sup>-/-</sup> and *Nrip1*<sup>+/+</sup> mice, which suggests that the increased thickness of sWAT in *Nrip1*<sup>-/-</sup> results from the increased number of cells. This is consistent with the reduced senescence and apoptosis detected in vitro and in vivo. Interestingly, we found that the diameter data of old B6 mice and old *Nrip1*<sup>+/+</sup> mice showed significant difference, which emphasizes the importance of using littermate controls in our study. Importantly, the aging-related inflammatory

**Fig. 8** Cell phenotypes of ADMSCs from middle age *Nrip1<sup>+/+</sup>* and *Nrip1<sup>-/-</sup>* mice. **a** cPDL of *Nrip1<sup>+/+</sup>* and *Nrip1<sup>-/-</sup>* ADMSCs passaged every 5 days. **b** qRT-PCR examined the expression of *p16*, *p21*, and *p53* in *Nrip1<sup>+/+</sup>* and *Nrip1<sup>-/-</sup>* ADMSCs at passage 3. **c** The level of IL-6 in *Nrip1<sup>+/+</sup>* and *Nrip1<sup>-/-</sup>* ADMSCs at passage 3. \* $P < 0.05$



cytokines *p65*, *IL1a*, and *IL6* are also significantly reduced. These results indicate that suppression of *Nrip1* may delay the skin aging in female mice.

To further investigate the role of NRIP1 in skin aging by regulating cellular senescence, we performed an in vitro study in ADMSCs isolated from sWAT. It has been reported that mouse ADMSCs could positively express CD29, CD44, and CD90 and did not express CD31, CD34, and CD45. Our FACS results showed that ADMSCs were positive for CD29 and CD44 and negative for CD31, which helped to verify the ADMSCs. Due to the differentiation potential, paracrine, and immunoregulation effects, ADMSCs have been reported to be utilized in dermatological applications such as facial atrophy, scars, wound healing, and alopecia [9]. Recent studies also revealed that injection of ADMSCs can prevent skin aging phenotype by stimulating collagen synthesis and increasing angiogenesis [19]. In our study, ADMSCs from *Nrip1<sup>-/-</sup>* mice showed reduced senescence in cell senescence assay compared to ADMSCs from *Nrip1<sup>+/+</sup>* mice. Likewise, ADMSCs from B6 mice treated by *siNrip1* also showed fewer senescent cells compared to *siCon*-treated ADMSCs. Cellular senescence is defined as a state of stable cell

cycle arrest due to diverse stresses, which is characterized by several molecular markers, including CDKIs (p16, p21) and p53 [21, 33]. It is well-known that senescence relies on two main molecular pathways: p53 and p16 pathways. As a tetrameric transcription factor, p53 is activated by several posttranslational modifications. Active p53 regulates the downstream pro-senescence target p21, which is responsible for G1 cell cycle arrest [32]. Once activated, the cyclin-dependent kinase (CDK) inhibitor p21 suppresses the activity of CDK2 and results in hypo-phosphorylated retinoblastoma protein (pRB), contributing to the onset of cellular senescence [14]. Furthermore, it has been reported that p16-positive cells accumulate during aging in multiple tissues [39]. The p16-mediated senescence also relies on controlling the pRB and leads to G1 cell cycle arrest [30]. Activated p16 prevents CDK4/6 from binding cyclin D and phosphorylating pRB. Otherwise, the phosphorylated pRB dissociates from the transcription factor E2F1, which allows E2F1 to enter the nucleus and to promote the transcription of target genes [23]. Another important phenotype of senescent cells is SASP, including *IL1a* and *IL6*. In the process of skin aging, senescent preadipocytes accumulate in

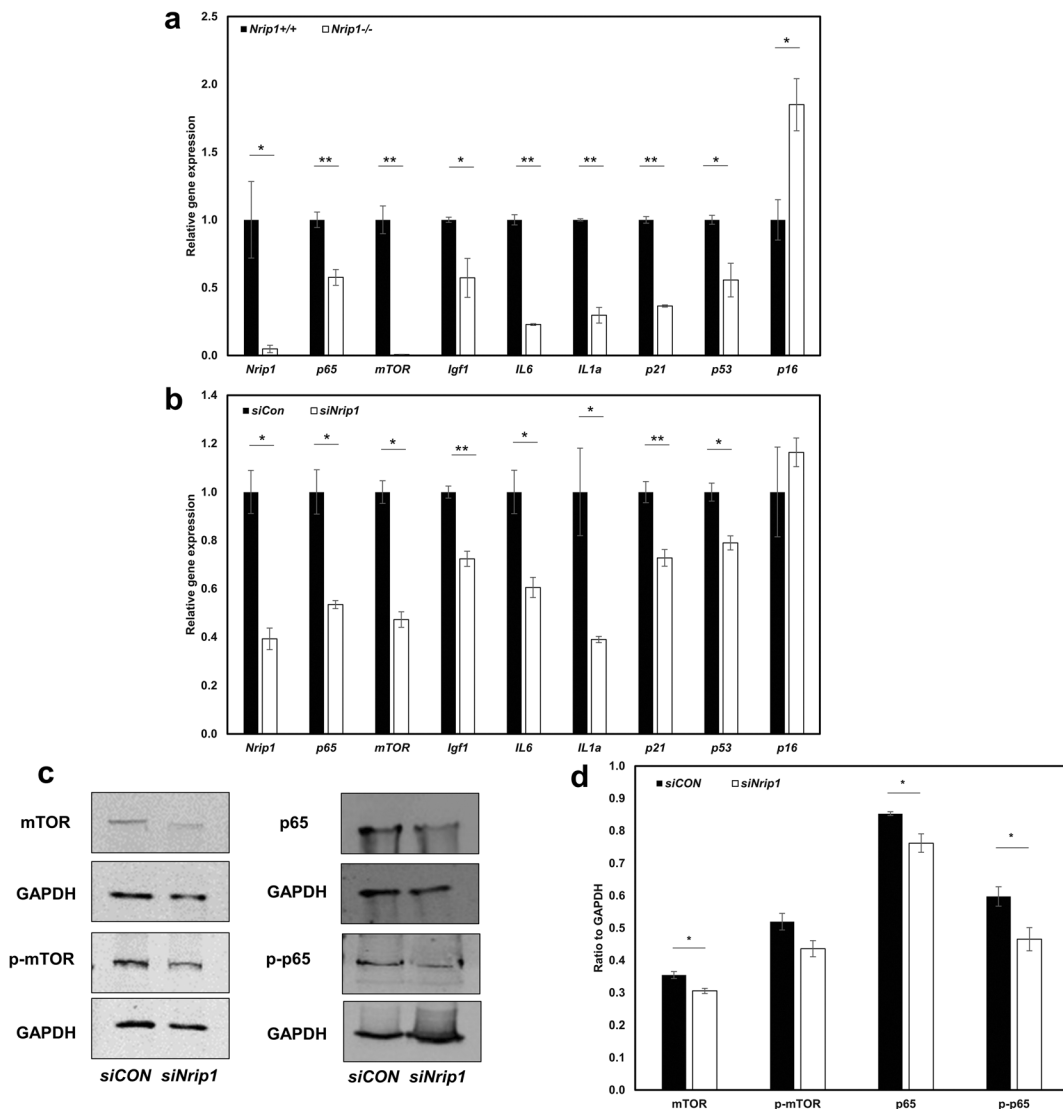


**Fig. 9** Depletion of *Nrip1* alters expression of senescence- and inflammation-associated genes. **a** qRT-PCR verified the deletion of *Nrip1* and examined the expression of senescence-associated genes (*p16*, *p21*, and *p53*), growth factors (*mTOR* and *Igf1*), and inflammation-related genes (*p65*, *IL6*, and *IL1a*) in *Nrip1*<sup>+/+</sup> and *Nrip1*<sup>-/-</sup> ADMSCs. **b** qRT-PCR verified the deletion of *Nrip1* and

examined the expression of senescence-associated genes (*p16*, *p21*, and *p53*), growth factors (*mTOR* and *Igf1*), and inflammation-related genes (*p65*, *IL6*, and *IL1a*) in *siCon* and *siNrip1* ADMSCs isolated from B6 mice. **c**, **d** Western blot quantification of mTOR, p-mTOR, p65, and p-p65 in *siCon* and *siNrip1* ADMSCs isolated from B6 mice. \**P*<0.05, \*\**P*<0.01

adipose tissue and secrete high levels of inflammatory cytokines [36]. Consistent with these findings, our results showed that the expressions of senescence-associated genes (*p21* and *p53*) and SASP (*IL1a* and *IL6*) are decreased in both *Nrip1*<sup>-/-</sup> and *siNrip1* ADMSCs compared to *Nrip1*<sup>+/+</sup> and *siCon* ADMSCs. Taken together, our results suggest that the deletion of *Nrip1* suppresses senescence not only in vivo in sWAT but also in vitro in ADMSCs.

Surprisingly, the expression of *p16* increased in *Nrip1*<sup>-/-</sup> ADMSCs compared to *Nrip1*<sup>+/+</sup> ADMSCs in the current study. Although *p16* is a key gene associated with senescence, it is reported that *p16* is also involved in regulating cell quiescence and apoptosis in mammalian cells. It is suggested that the level of *p16* is elevated in quiescent smooth muscle cell in rat aorta [16]. Likewise, *p16* prevents dentate gyrus stem cells from being activated and contributes to the maintenance of cell

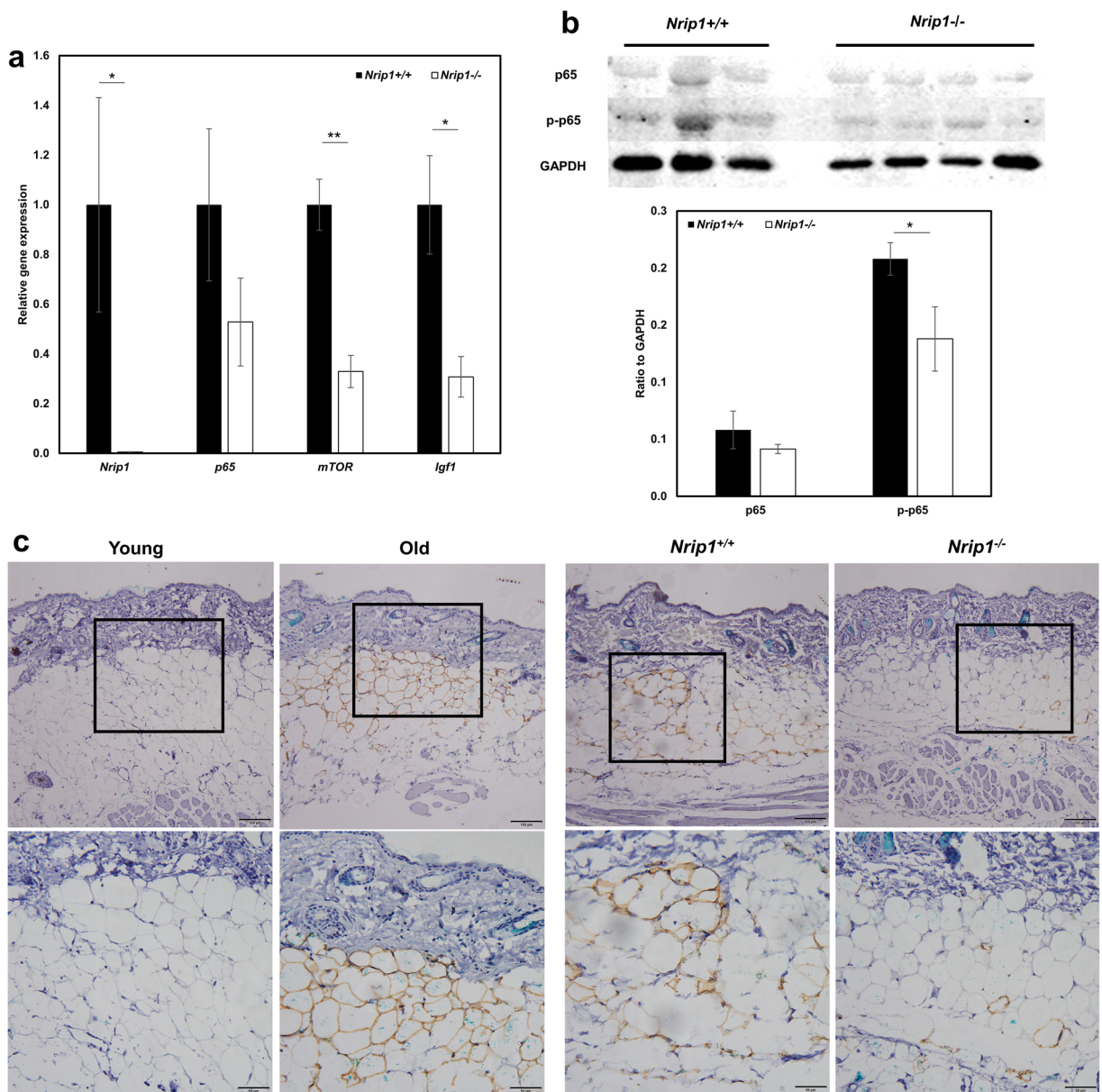


**Fig. 10** Depletion of *Nrip1* reduces p-p65 level in skin. **a** qRT-PCR verified the deletion of *Nrip1* and examined the expression of *p65*, *mTOR*, and *Igf1* in skin of *Nrip1*<sup>+/+</sup> and *Nrip1*<sup>-/-</sup> mice. **b** Western blot quantification of p65 and p-p65 in skin of *Nrip1*<sup>-/-</sup>

and *Nrip1*<sup>+/+</sup> mice. **c** Immunohistochemical detection of p-p65 expression in young and old B6 mice, as well as in *Nrip1*<sup>-/-</sup> and *Nrip1*<sup>+/+</sup> mice at old age (upper scale bar 100μm, down scale bar 50μm). \**P*<0.05, \*\**P*<0.01

quiescence by reserving the self-renewal capacity [28]. RB-E2F signaling plays a vital role in stem cell quiescence as E2F is suppressed by the binding of RB in quiescent cells. Moreover, Rb has been shown to have a specialized role in regulating cell cycle exit [4]. Recent studies have raised a model controlling the conversion of quiescence and proliferation which is called “RB-E2F bistable switch.” The “E2F off” (quiescence) state

means that cells remain in the reversible G0 state when E2F is suppressed. The “E2F on” (proliferation) state means that cells re-enter the G1 of cell cycle when E2F is activated [42]. As we mentioned before, the binding of p16 with CDK4/6 could result in the reduced levels of E2F1 released from the Rb [30]. Together, these studies suggest that p16 functions as an inhibition factor of E2F1 and leads to the “E2F off” state which cells remain

quiescent. Additionally, P16 may also act as an inhibitor of DNA damage-induced apoptosis and can protect cells from UV-dependent apoptosis by regulating the expression of Bcl-2 [1]. Therefore, in our study, inhibited apoptosis in ADMSCs by NRIP1 deletion may also be related to the elevated expression of p16. However, the elevated P16 needs to be further verified at the protein level and its effects on stromal cell quiescence and apoptosis needs to be further investigated.

Although ADMSCs are considered to have strong self-renewal and cell proliferation capability, several studies have shown that the function of ADMSCs decreases with aging. The cell morphology, proliferation capability, and differentiation potential of ADMSCs from old donors are significantly different from ADMSCs from young donors, which may limit the therapeutic potential of ADMSCs [6]. Therefore, improving the function of ADMSCs by genetic treatment may provide a new approach for better clinical outcomes. To investigate the effects of NRIP1 on the cellular function of ADMSCs, we tested cell proliferation, apoptosis, and differentiation. Our results showed that ADMSCs from *Nrip1*<sup>-/-</sup> mice have impaired proliferation and less apoptosis compared to ADMSCs from *Nrip1*<sup>+/+</sup> mice. Our previous data found that suppressing NRIP1 inhibited cell growth and induced apoptosis in breast cancer cell lines [3]. Indeed, we used the primary ADMSCs as the target cell type in our current study, which have the unique cell quiescent state compared to the cancer cell lines. Interestingly, the quiescent stem cells show decreased differentiation and apoptosis [38]. Regarding the adipogenic differentiation, the lipid droplet accumulation measured by Oil Red assay revealed a significant decrease in *Nrip1*<sup>-/-</sup> ADMSCs compared to *Nrip1*<sup>+/+</sup> ADMSCs. Furthermore, the same trend was observed in the quantitative analysis of molecular markers of adipogenic differentiation (*Fabp4*, *Pppar* $\gamma$ , and *Adiponectin*). Apart from the vital role in senescence, p53 also takes part in the maintenance of stem cells by acting as a differentiation regulator. Studies have shown that activation of p53 can lead to the rapid differentiation of human embryonic stem cells, and knocking out p53 can delay the differentiation [17, 27]. Consistent with these findings, our results indicate that suppressing *Nrip1* can decrease the expression of p53 and inhibit adipogenic differentiation. Taken together, these assays show that suppression of *Nrip1* leads to reduced proliferation, decreased apoptosis, and adipogenic differentiation.

To understand the reason why depletion of *Nrip1* can reduce cell senescence, decrease cell proliferation, prevent cell apoptosis, and decrease adipogenic differentiation potential, we hypothesize cell cycle and quiescence of ADMSC as possible underlying mechanisms. As expected, our results showed that the quiescent cells in ADMSCs from *Nrip1*<sup>-/-</sup> mice were significantly increased compared to ADMSCs from *Nrip1*<sup>+/+</sup> mice. Cellular quiescence is the reversible state in which cells exist in the G0 stage of cell cycle and stay as dormant with low-activity [38]. For mammalian stem cells, quiescence can preserve self-renewal, proliferation, and differentiation, which is critical for survival and long-term reconstituting capacity [22]. Based on the unique characteristics of stem cell quiescence, two innovative therapeutic strategies have been established which could provide promising clinical outcomes in the near future. The first is called “lock-out” strategy, which consists of pushing stem cells out of quiescence to induce proliferation and differentiation. The other one is called “lock-in” strategy, which consists of maintaining the quiescent state to prevent aberrant proliferation and differentiation or premature senescence [5]. According to these findings and our results, we believe that depletion of *Nrip1* could lead to ADMSCs maintaining a quiescent cell cycle state to preserve their long-term function and self-renewal capacity.

To further confirm our hypothesis that ADMSCs could preserve their long-term function by maintaining cell quiescence, we investigated the cell phenotypes of ADMSCs from middle age *Nrip1*<sup>+/+</sup> and *Nrip1*<sup>-/-</sup> mice. We noticed an interesting phenomenon that the proliferation rate of *Nrip1*<sup>-/-</sup> ADMSCs at middle age was higher than that of *Nrip1*<sup>+/+</sup> ADMSCs based on the cPDL result. The expression of cyclin-dependent kinase (p21 and p53) was significantly lower in *Nrip1*<sup>-/-</sup> ADMSCs compared to *Nrip1*<sup>+/+</sup> ADMSCs. The level of SASP marker (IL-6) was also significantly lower in *Nrip1*<sup>-/-</sup> ADMSCs compared to *Nrip1*<sup>+/+</sup> ADMSCs. According to these results, we found that *Nrip1*<sup>+/+</sup> ADMSCs at middle age began senescing earlier than *Nrip1*<sup>-/-</sup> ADMSCs, which suggests that as early as middle age the *Nrip1*<sup>-/-</sup> ADMSCs may function better than *Nrip1*<sup>+/+</sup> ADMSCs. Combined with our previous findings, it is reasonable to conclude that deletion of *Nrip1* could maintain ADMSCs quiescence and preserve the stem cell ability at young age, thus reducing ADMSCs senescence during aging.

Although the underlying mechanism of how NRIP1 regulates ADMSCs quiescence is unclear, our current results showed that the expression of mTOR is significantly decreased not only in the ADMSCs from *Nrip1*<sup>-/-</sup> mice but also in *siNrip1*-treated ADMSCs. The accumulating data have shown a strong association between mTOR and stem cell quiescence. It has been reported that mTOR activity is necessary for the transition of stem cells from G0 into G(Alert), where G(Alert) stem cells have higher priority to enter cell cycle [31]. Various genetic studies have demonstrated that deletion of several mTOR-negative regulators, including TSC1, PTEN, PML, and Fbxw7, could result in hyperproliferation and subsequent exhaustion, and defective repopulating potential, which means these mTOR-negative regulators could maintain stem cell quiescence [8]. Furthermore, mTOR signaling has been reported to possess a deleterious role on stem cell maintenance during repeated regeneration cycles [11]. It has been proposed that pharmacological inhibition of mTOR by rapamycin and metformin is sufficient for stem cells to maintain a quiescent state [29]. Based on these findings and our current data, it is suggested that suppressing NRIP1 could maintain ADMSC quiescence by inhibiting mTOR.

As one of the key mediators of aging, increased NFκB activity during skin aging has been observed in several studies [13, 15, 37]. In accordance with this, we found the level of p65 was increased in the sWAT at old age of B6 mice. More importantly, our data firstly demonstrated that the deletion of *Nrip1* could reduce the expression of p65 and p-p65 in both skin and ADMSCs. Our previous studies also reported that knocking down *Nrip1* can significantly reduce the expression of NFκB in both human keratinocytes and periovarian WAT [26, 40]. Although the underlying mechanism of how NRIP1 regulates NFκB/p65 is unclear, our current results showed that the expression of *Igf1* is significantly decreased not only in the skin of *Nrip1*<sup>-/-</sup> mice but also in *Nrip1*<sup>-/-</sup> and *siNrip1* ADMSCs. It has been proposed that IGF1 can activate the downstream PI-3K and Akt, which in turn enhance the NFκB signaling via the IKK complex [34, 37]. In the canonical NFκB signaling pathway, the dimer of p65 and p50 is in an inactive state by the inhibition of IκB in cytoplasm. Upon stimulation, IKKs phosphorylate IκB, which results in their degradation and enables NFκB translocate to the nucleus to induce target gene expression [24]. Given the fact that depletion of NRIP1 leads to the

decreased expression of IGF1 and NFκB and reduced level of p65, it is reasonable to conclude that NRIP1 may regulate skin aging through the IGF1/ NFκB pathway.

In conclusion, our results revealed that NRIP1 plays a significant role in skin aging. Deletion of *Nrip1* can delay skin aging phenotypes, reduce ADMSCs senescence, and maintain ADMSCs quiescence. This suggests that NRIP1 might be a potential therapeutic target to improve the function of ADMSCs and contribute to delayed skin aging.

**Acknowledgments** Lisa Hensley kindly edited the manuscript. Division of Laboratory Animal Medicine of Southern Illinois University School of Medicine provides excellent environment for animal research.

**Author contributions** RY conceived and designed the project; YH, YZ, SDG, and JMO performed the experiments; RY, YH, YZ, and SDG analyzed experimental results; YH and RY wrote the manuscript with approval from all authors; RY, HG, and MC revised the manuscript.

**Funding** The work is funded by U.S. NIH grant AG046432, internal research seed grants of Southern Illinois University School of Medicine, team science grant of simmons cancer institute at Southern Illinois University School of Medicine, CAMS Innovation Fund for Medical Sciences (CIFMS-2017-I2M-1-017), and China Scholarship Council (No. 201806210434).

**Declarations**

**Conflict of interest** The authors declare no competing interests.

## References

1. Al-Mohanna MA, Manogaran PS, Al-Mukhalafi Z, Al-Hussein KA, Aboussekhra A. The tumor suppressor p16(INK4a) gene is a regulator of apoptosis induced by ultraviolet light and cisplatin. *Oncogene*. 2004;23:201–12. <https://doi.org/10.1038/sj.onc.1206927>.
2. Augereau P, Badia E, Carascossa S, Castet A, Fritsch S, Harmand PO, et al. The nuclear receptor transcriptional coregulator RIP140. *Nucl Recept Signal*. 2006;4:e024. <https://doi.org/10.1621/nrs.04024>.
3. Aziz MH, Chen X, Zhang Q, DeFrain C, Osland J, Luo Y, et al. Suppressing NRIP1 inhibits growth of breast cancer cells in vitro and in vivo. *Oncotarget*. 2015;6:39714–24. <https://doi.org/10.18632/oncotarget.5356>.
4. Biggar KK, Storey KB. Perspectives in cell cycle regulation: lessons from an anoxic vertebrate. *Curr Genomics*. 2009;10: 573–84. <https://doi.org/10.2174/138920209789503905>.

5. Cho JJ, Lui PP, Obajdin J, Riccio F, Stroukov W, Willis TL, et al. Mechanisms, Hallmarks, and Implications of Stem Cell Quiescence. *Stem Cell Rep.* 2019;12:1190–200. <https://doi.org/10.1016/j.stemcr.2019.05.012>.
6. Faffian-Labora JA, Morente-Lopez M, Arufe MC. Effect of aging on behaviour of mesenchymal stem cells. *World J Stem Cells.* 2019;11:337–46. <https://doi.org/10.4252/wjsc.v11.i6.337>.
7. Flurkey K, Yuan R. How the evolutionary theory of aging can guide us in the search for aging genes. *Aging (Albany NY).* 2012;4:318–9. <https://doi.org/10.18632/aging.100460>.
8. Gan B, DePinho RA. mTORC1 signaling governs hematopoietic stem cell quiescence. *Cell Cycle.* 2009;8:1003–6. <https://doi.org/10.4161/cc.8.7.8045>.
9. Gaur M, Dobke M, Lunyak VV. Mesenchymal Stem Cells from Adipose Tissue in Clinical Applications for Dermatological Indications and Skin Aging. *Int J Mol Sci.* 2017;18. <https://doi.org/10.3390/ijms18010208>.
10. Ghosh S, Thakur MK. Tissue-specific expression of receptor-interacting protein in aging mouse. *Age (Dordr).* 2008;30:237–43. <https://doi.org/10.1007/s11357-008-9062-3>.
11. Haller S, Kapuria S, Riley RR, O’Leary MN, Schreiber KH, Andersen JK, et al. mTORC1 Activation during Repeated Regeneration Impairs Somatic Stem Cell Maintenance. *Cell Stem Cell.* 2017;21:806–18 e805. <https://doi.org/10.1016/j.stem.2017.11.008>.
12. Harkema L, Youssef SA, de Bruin A. Pathology of Mouse Models of Accelerated Aging. *Vet Pathol.* 2016;53:366–89. <https://doi.org/10.1177/0300985815625169>.
13. Haustead DJ, Stevenson A, Saxena V, Marriage F, Firth M, Silla R, et al. Transcriptome analysis of human ageing in male skin shows mid-life period of variability and central role of NF-kappaB. *Sci Rep.* 2016;6:26846. <https://doi.org/10.1038/srep26846>.
14. Herranz N, Gil J. Mechanisms and functions of cellular senescence. *J Clin Invest.* 2018;128:1238–46. <https://doi.org/10.1172/JCI95148>.
15. Hu Y, Zhu Y, Lian N, Chen M, Bartke A, Yuan R. Metabolic Syndrome and Skin Diseases. *Front Endocrinol (Lausanne).* 2019;10. <https://doi.org/10.3389/fendo.2019.00788>.
16. Izzard TD, Taylor C, Birkett SD, Jackson CL, Newby AC. Mechanisms underlying maintenance of smooth muscle cell quiescence in rat aorta: role of the cyclin dependent kinases and their inhibitors. *Cardiovasc Res.* 2002;53:242–52. [https://doi.org/10.1016/S0008-6363\(01\)00444-8](https://doi.org/10.1016/S0008-6363(01)00444-8).
17. Jain AK, Allton K, Iacovino M, Mahen E, Milczarek RJ, Zwaka TP, et al. p53 regulates cell cycle and microRNAs to promote differentiation of human embryonic stem cells. *PLoS Biol.* 2012;10:e1001268. <https://doi.org/10.1371/journal.pbio.1001268>.
18. Khavkin J, Ellis DA. Aging skin: histology, physiology, and pathology. *Facial Plast Surg Clin North Am.* 2011;19:229–34. <https://doi.org/10.1016/j.fsc.2011.04.003>.
19. Kim J-H, Jung M, Kim H-S, Kim Y-M, Choi E-H. Adipose-derived stem cells as a new therapeutic modality for ageing skin. 2011;20:383–7. <https://doi.org/10.1111/j.1600-0625.2010.01221.x>.
20. Kohl E, Steinbauer J, Landthaler M, Szeimies RM. Skin ageing. *J Eur Acad Dermatol Venereol.* 2011;25:873–84. <https://doi.org/10.1111/j.1468-3083.2010.03963.x>.
21. Kuilman T, Michaloglou C, Mooi WJ, Peeper DS. The essence of senescence. *Genes Dev.* 2010;24:2463–79. <https://doi.org/10.1101/gad.1971610>.
22. Li L, Bhatia R. Stem cell quiescence. *Clin Cancer Res.* 2011;17:4936–41. <https://doi.org/10.1158/1078-0432.CCR-10-1499>.
23. Liu JY, Souroullas GP, Diekmann BO, Krishnamurthy J, Hall BM, Sorrentino JA, et al. Cells exhibiting strong p16 (INK4a) promoter activation in vivo display features of senescence. *Proc Natl Acad Sci U S A.* 2019;116:2603–11. <https://doi.org/10.1073/pnas.1818313116>.
24. Liu T, Zhang L, Joo D, Sun SC. NF-kappaB signaling in inflammation. *Signal Transduct Target Ther.* 2017;2. <https://doi.org/10.1038/sigtrans.2017.23>.
25. Lopez-Lluch G, Irusta PM, Navas P, de Cabo R. Mitochondrial biogenesis and healthy aging. *Exp Gerontol.* 2008;43:813–9. <https://doi.org/10.1016/j.exger.2008.06.014>.
26. Luan C, Chen X, Hu Y, Hao Z, Osland JM, Chen X, et al. Overexpression and potential roles of NRIP1 in psoriasis. *Oncotarget.* 2016;7:74236–46. <https://doi.org/10.18632/oncotarget.12371>.
27. Maimets T, Neganova I, Armstrong L, Lako M. Activation of p53 by nutlin leads to rapid differentiation of human embryonic stem cells. *Oncogene.* 2008;27:5277–87. <https://doi.org/10.1038/nc.2008.166>.
28. Micheli L, D’Andrea G, Ceccarelli M, Ferri A, Scardigli R, Tirone F. p16Ink4a Prevents the Activation of Aged Quiescent Dentate Gyrus Stem Cells by Physical Exercise. *Front Cell Neurosci.* 2019;13:10. <https://doi.org/10.3389/fncel.2019.00010>.
29. Pavlidou T, Marinkovic M, Rosina M, Fuoco C, Vumbaca S, Gargioli C, et al. Metformin Delays Satellite Cell Activation and Maintains Quiescence. *Stem Cells Int.* 2019;2019:5980465–19. <https://doi.org/10.1155/2019/5980465>.
30. Rayess H, Wang MB, Srivatsan ES. Cellular senescence and tumor suppressor gene p16. *Int J Cancer.* 2012;130:1715–25. <https://doi.org/10.1002/ijc.27316>.
31. Rodgers JT, King KY, Brett JO, Cromie MJ, Charville GW, Maguire KK, et al. mTORC1 controls the adaptive transition of quiescent stem cells from G0 to G(Alert). *Nature.* 2014;510:393–6. <https://doi.org/10.1038/nature13255>.
32. Rufini A, Tucci P, Celardo I, Melino G. Senescence and aging: the critical roles of p53. *Oncogene.* 2013;32:5129–43. <https://doi.org/10.1038/nc.2012.640>.
33. Salama R, Sadaie M, Hoare M, Narita M. Cellular senescence and its effector programs. *Genes Dev.* 2014;28:99–114. <https://doi.org/10.1101/gad.235184.113>.
34. Salminen A, Kaamiranta K. Insulin/IGF-1 paradox of aging: regulation via AKT/IKK/NF-kappaB signaling. *Cell Signal.* 2010;22:573–7. <https://doi.org/10.1016/j.cellsig.2009.10.006>.
35. Schosserer M, Grillari J, Wolfrum C, Scheideler M. Age-Induced Changes in White, Brite, and Brown Adipose Depots: A Mini-Review. *Gerontology.* 2018;64:229–36. <https://doi.org/10.1159/000485183>.

36. Starr ME, Saito M, Evers BM, Saito H. Age-Associated Increase in Cytokine Production During Systemic Inflammation-II: The Role of IL-1beta in Age-Dependent IL-6 Upregulation in Adipose Tissue. *J Gerontol A Biol Sci Med Sci*. 2015;70:1508–15. <https://doi.org/10.1093/gerona/glu197>.
37. Tilstra JS, Clauson CL, Niedernhofer LJ, Robbins PD. NF-kappaB in Aging and Disease. *Aging Dis*. 2011;2:449–65.
38. van Velthoven CTJ, Rando TA. Stem Cell Quiescence: Dynamism, Restraint, and Cellular Idling. *Cell Stem Cell*. 2019;24:213–25. <https://doi.org/10.1016/j.stem.2019.01.001>.
39. Wang AS, Dreesen O. Biomarkers of Cellular Senescence and Skin Aging. *Front Genet*. 2018;9:247. <https://doi.org/10.3389/fgene.2018.00247>.
40. Wang J, Chen X, Osland J, Gerber SJ, Luan C, Delfino K, et al. Deletion of Nrip1 Extends Female Mice Longevity, Increases Autophagy, and Delays Cell Senescence. *J Gerontol A Biol Sci Med Sci*. 2018;73:882–92. <https://doi.org/10.1093/gerona/glx257>.
41. Wollina U, Wetzker R, Abdel-Naser MB, Kruglikov IL. Role of adipose tissue in facial aging. *Clin Interv Aging*. 2017;12:2069–76. <https://doi.org/10.2147/CIA.S151599>.
42. Yao G. Modelling mammalian cellular quiescence. *Interface Focus*. 2014;4:20130074. <https://doi.org/10.1098/rsfs.2013.0074>.
43. Zouboulis CC, Makrantonaki E. Clinical aspects and molecular diagnostics of skin aging. *Clin Dermatol*. 2011;29:3–14. <https://doi.org/10.1016/j.clindermatol.2010.07.001>.
44. Zschiedrich I, Hardeland U, Krones-Herzig A, Berriel Diaz M, Vegiopoulos A, Muggenburg J, et al. Coactivator function of RIP140 for NFkappaB/RelA-dependent cytokine gene expression. *Blood*. 2008;112:264–76. <https://doi.org/10.1182/blood-2007-11-121699>.

**Publisher's note** Springer Nature remains neutral with regard to jurisdictional claims in published maps and institutional affiliations.